ELSEVIER

Ceramics International 30 (2004) 333–342

CERAMICS
INTERNATIONAL

www.elsevier.com/locate/ceramint

Microstructure and properties of zirconia-based nanocomposites derived from a powder containing TiC crystallised in situ and carbon

Waldemar Pyda*

AGH University of Science and Technology, Faculty of Materials Science and Ceramics, Department of Special Ceramics,
al. Mickiewicza 30, 30-059 Cracow, Poland

Received 8 January 2003; received in revised form 27 January 2003; accepted 4 May 2003

Abstract

The reaction between carbon and titanium originated from zirconia–titania solid solution was used to produce TiC inclusions in situ in zirconia powders and dense materials. The co-precipitated powder composed of 1.5 mol% Y_2O_3, 18 mol% TiO_2 and 80.5 mol% ZrO_2 was mixed with phenol-formaldehyde resin in an amount giving 200% excess of carbon in terms of the stoichiometry of the carbothermal reduction of TiO_2. The mixture was heated for 2 h at 1500 °C in argon. The resultant composite powder was composed mainly of tetragonal and monoclinic phases and contained 9 wt.% TiC and non-reacted carbon. The mixture of the composite powder and the original co-precipitated one (25/75 wt.%) was used to prepare composite materials by means of pressureless sintering in argon. The sintered bodies were composed mainly of tetragonal and monoclinic phase and contained nanocrystalline TiC inclusions which showed two different morphologies: oval and elongated. The role of oxygen vacancies in the in situ formation of the elongated TiC inclusions is discussed. Improvement in the characteristics of the zirconia materials was obtained.

Keywords: A. Powders: solid state reaction; B. Nanocomposites; B. Inclusions; D. ZrO_2; D. Carbides

1. Introduction

Among numerous papers dealing with the incorporation of inclusions into the Y-TZP matrix [1–7] in order to improve its hardness, fracture toughness, high-temperature strength or thermal conductivity, few concentrate on the preparation and properties of ZrO_2–TiC ceramic matrix composites [8–13]. Two ways of preparation of the composites can be distinguished: (i) physical mixing of the constituent powders [8–10], (ii) utilising the reaction between carbon and titanium dissolved within the zirconia solid solution to produce in situ TiC inclusions [11–13]. The former way yields composites with micrometric size inclusions, the latter one is especially suitable for the preparation of nanocomposites.

Fukuhara [8] studied the effect of TiC addition on the properties of an Y–TZP–Al_2O_3 composite ceramic. The co-precipitated powder composed of 20 wt.% Al_2O_3 and 80 wt.% ZrO_2 stabilized with 2.5 mol% Y_2O_3 was physically mixed with a commercial TiC powder. The strength of the isostatically hot-pressed composites (0.5 h at 1700 °C and 168 MPa in argon) was found to increase with addition of TiC above 10 wt.%, showing a maximum value (~1.4 GPa) at ≈30 wt.% TiC. Adding TiC to the binary ceramic suppressed the decrease in strength above 1300 °C and improved the hardness, fracture toughness, and electrical conductivity at room temperature.

Zhan et al. [9] studied the Y–TZP ceramics containing up to 30 vol.% TiC particles. A physical mixture of the 3 mol% Y_2O_3–ZrO_2 powder with the TiC one was used. The cold isostatically pressed compacts were hot-pressed for 40 min at 1700 °C under 30 MPa in argon. Adding TiC particles to Y–TZP did not changed practically the bending strength and it improved the fracture toughness and hardness. With 20 vol.% TiC particles the bending strength, fracture toughness and Vickers hardness of the composites reached ~1.1 GPa, 14.6

---

* Tel.: +48-12-617-23-97.
E-mail address: pyda@uci.agh.edu.pl (W. Pyda).

0272-8842/03/$30.00 © 2003 Elsevier Ltd and Techna S.r.l. All rights reserved.
doi:10.1016/S0272-8842(03)00105-6

MPa·m$^{0.5}$ and 16.0 GPa, respectively. Both authors have found that additions of less than 10 vol.% TiC caused the sintered density and strength to decrease dramatically. This has been attributed to gaseous species evolved due to the reaction between zirconia and TiC.

Vleugels et al. [10] studied a ZrO_2–TiC (70/30 vol.%) composite prepared from a physical mixture of commercially available ZrO_2 with 2.77 mol% Y_2O_3 and TiC powders. The bending strength of the ZrO_2–TiC composite hot-pressed under 28 MPa for 1 h at 1450 °C showed a smaller value (750 MPa) than that measured for the Y–TZP matrix (950 MPa).

The author's preliminary attempt at the in situ synthesis of TiC inclusions in a zirconia matrix has been reported in Ref. [11]. The method was based on the assumption that Ti derived from a Y_2O_3–TiO_2–ZrO_2 solid solution can react with carbon introduced into the system to produce TiC inclusions. A co-precipitated powder of the zirconia solid solution stabilized with 1.5 mol% Y_2O_3 and 18 mol% TiO_2 and phenol-formaldehyde resin as a carbon source were used to prepare homogeneous mixtures that were pressureless heat treated in argon at 1400 or 1500 °C. The formation of TiC inclusions was confirmed. The composites with in situ grown TiC inclusions of $\sim$200 nm in size showed a promising increase in fracture toughness.

Using the same method Haberko et al. [12] prepared a TiC–TZP composite starting from a solid solution powder of composition 3 mol% Y_2O_3, 18 mol% TiO_2, and 79 mol% ZrO_2. The material, hot-pressed at 1500 °C under 25 MPa in argon, showed a density of +98%, a hardness of 17 GPa, a Young's modulus of 221 GPa and a fracture toughness of 4.1 MPa·m$^{0.5}$ in the presence of 8.3 vol.% TiC inclusions.

Liu et al. [13] prepared a zirconia powder containing TiC by carbonising the co-precipitated 3 mol% Y_2O_3–97 mol% ZrO_2+TiO_2 powder with sucrose for 2 h at 1450 °C in argon. The particle size of the carbonised powder was in the range of about 50–200 nm and most of the particles were spherical. Sintering behaviour of the powder was not studied.

Most commercial TiC is made by the carbothermal reduction of TiO_2 at 2000 °C or above in a hydrogen atmosphere according to the overall reaction:

$$TiO_2(s) + 3C(s) \leftrightarrow TiC(s) + 2CO(g). \quad (1)$$

Thermodynamic calculations for the TiO_2–C system [14] indicate that TiO_2 can react with carbon to produce titanium carbide at temperatures higher than 1280 °C under a CO partial pressure of 1 atm. Lowering the CO partial pressure to $P_{CO} = 10^{-6}$ atm decreases the reaction temperature even to 1000 °C. The reaction corresponding to Eq. (1) has been assumed to operate during the in situ synthesis in the case of the powders of yttria–titania–zirconia solid solution treated with carbon [10,12]. However, some experimental results connected to the TiC in situ crystallization within dense zirconia polycrystals are difficult to explain in terms of the process, during which gaseous products are evolved at the reaction front and they need another approach. This concerns TiC-rich surface layers produced in dense Ti,Y–TZP by means of the reaction of carbon and titanium, reported by Haberko et al. [15], in which porosity connected to the CO evolution was not observed.

The aim of the present work was to produce dense nanocomposites in the TiC–ZrO_2 system using a zirconia–titania powder which contains TiC synthesized in situ when an excess of carbon is used and to characterise properties both of the starting powder and the resultant sintered bodies. For the first time, the mechanism of formation of the TiC inclusions is discussed.

2. Experimental

The flow chart for the experiment performed to prepare zirconia powders and sintered bodies with TiC inclusions is shown in Fig. 1. A co-precipitation and calcination method was used to prepare the powder of zirconia solid solution stabilized with 1.5 mol% Y_2O_3 and 18 mol% TiO_2 (sample Z). A zirconia–yttria–titania hydrogel was co-precipitated from an aqueous solution of appropriate chlorides with $NH_3·H_2O$ at a pH of 9. The following chemical reagents were used: $ZrOCl_2$– >99%, Y_2O_3– >99.99% and $TiCl_4$ >99%. The gel was washed with distilled water, dried and then calcined for 2 h at 700 °C.

Homogeneous mixture of the 1.5 mol% Y_2O_3–18 mol% TiO_2–80.5 mol% ZrO_2 powder and carbon was prepared using a solution (20%) of phenol-formaldehyde resin in ethanol (95 vol.%). The amount of carbon, which remained after the resin decomposition, came to 50 wt.%. The mixture contained 200% of carbon in terms of the stoichiometry of the reaction depicted with Eq. 1 (sample Z+200C). In order to synthesize the TiC-rich zirconia composite powder (sample Z+TiC), the Z+200C mixture was heated for 2 h at 1500 °C in a flow of technical argon (12 dm^3/h) purified from oxygen by active copper. A furnace with Superkanthal 1900 heating elements and a 6 °C/min rate of temperature increase was used. The Z+TiC powder was used to prepare composite materials. To do this, the mixture composed of 25 wt.% of Z+TiC and 75 wt.% of Z was milled for 3 h in ethanol in a rotation-vibration mill. Cold isostatically pressed green bodies (P=350 MPa) were sintered for 2 h at 1400 or 1500 °C in a carbon bed in the same furnace, heating conditions and atmosphere as in the case of the Z+TiC preparation.

X-ray analysis was applied to characterize the phase composition of the powders and sintered bodies. Scans were recorded from polished surfaces of the samples (1 μm diamond polishing powder) in the 25–80° 2Θ range using CuK_α radiation in steps of 0.02°. The pseudo-Voigt function was used to fit a profile shape of overlapping peaks. The evaluation of phase contents was made by the following formulas:

$$V_m = \frac{1.603 \cdot I(\bar{1}11)_m}{1.603 \cdot I(\bar{1}11)_m + I(111)_t} \text{ [16]} \tag{2}$$

$$W_{TiC} = 1.54(\pm 0.06) \times \frac{I(111)_{TiC} + I(200)_{TiC}}{I(\bar{1}11)_m + I(111)_t + I(111)_m + I(111)_{TiC} + I(200)_{TiC}} \tag{3}$$

$$V_m + V_{TiC} + V_t = 1 \tag{4}$$

where: V_m, V_t and V_{TiC} denotes volume fractions of monoclinic zirconia, tetragonal zirconia, and TiC, respectively, W_{TiC} weight fraction of TiC, I—integral intensity of the indicated peak of the monoclinic, m, tetragonal, t, zirconia and titanium carbide, TiC, phases. The proportionality factor in the formula (3) has been derived from integral intensity measurements, performed for mixtures of TiC (HCST 2575, Herman C. Starck, Berlin, Germany) and 3Y-TZP (TOSOH, Japan) powders with known composition (3–12 wt.%). The conversion from weight to volume fraction of TiC was made assuming the density of TiC to be 4.93 g/cm^3 and that of ZrO_2 s.s. to be 6.0 g/cm^3. Cell parameters of TiC synthesized in situ were also assessed from the above X-ray measurements.

Transmission and scanning electron microscopy were applied to observe the morphology of the powders and the microstructure of the sintered bodies, respectively. Fracture toughness, K_{Ic}, was determined on polished surfaces by Vickers' indentation, using the Palmqvist crack model [17]. The density was determined by the Archimedes' method.

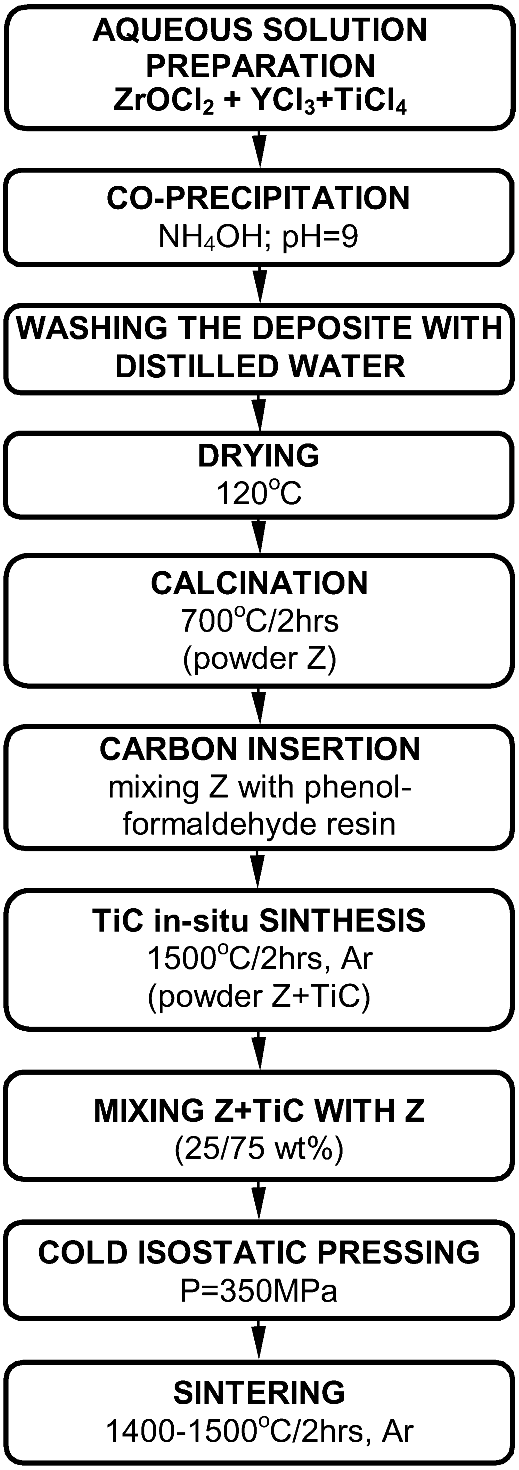

Fig. 1. Preparation route of powders and zirconia bodies with TiC inclusions.

3. Results and discussion

3.1. Characteristics of the powders

The calcination of the zirconia–yttria–titania gel resulted in the powder of morphology shown in Fig. 2 a. Agglomerates of the Z powder were composed of nanometric (~20 nm), isometric crystallites. The phase of tetragonal symmetry dominated that of monoclinic symmetry as indicated by the data of Table 1 and Fig. 3.

The Z+200C mixture heated for 2 h at 1500 °C in argon, showed crystallites with the increased size (~0.3 μm) and mostly plate-shaped morphology (Fig. 2b), decreased amount of the monoclinic phase and a TiC content of 9 wt.% (Table 1) as measured by XRD. This value corresponds well with the value of 9.51 wt.% which represents the maximum expected concentration of stoichiometric TiC when the total amount of Ti

Table 1
Properties of powders

Property	Z	Z + TiC as synthesized	Z + TiC milled
Specific surface area, m^2/g	68.4±1.2	105.6	108.5
Monoclinic phase content, vol.%	19.2±0.5	15.3±0.2	35.4±0.4
Tetragonal phase content, vol.%	80.8±0.5	74.0±0.2	53.5±0.2
TiC content, wt.%	0	9.0±0.2	9.3±0.1
TiC content, vol.%	0	10.8±0.2	11.1±0.2

±Denotes confidence interval at confidence level of 0.95 in the entire work.

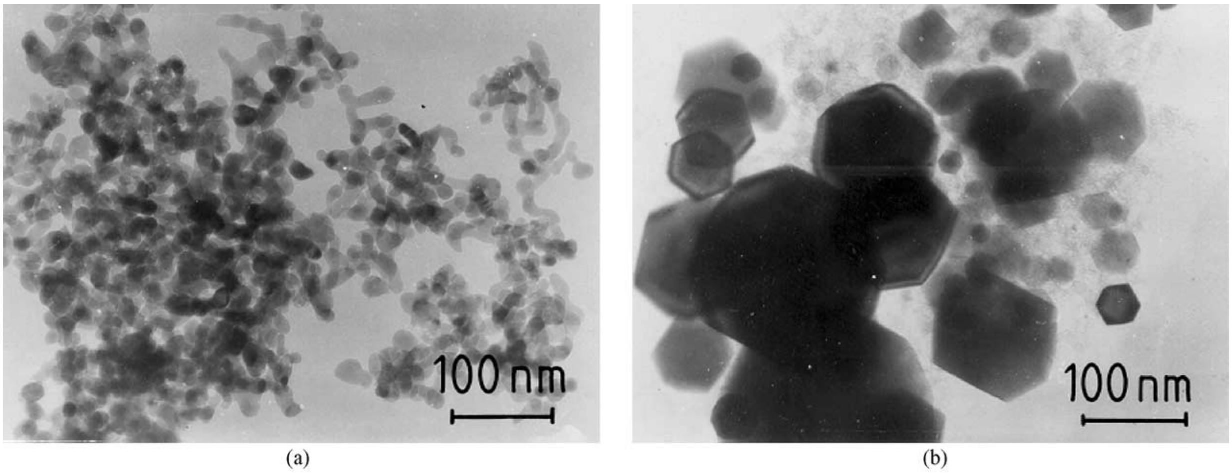

(a) (b)

Fig. 2. TEM microphotographs of the powders: (a) original powder calcined for 1 h at 700 °C in air (sample Z), (b) Z + 200C mixture heat treated for 1 h at 1500 °C in argon (sample Z + TiC).

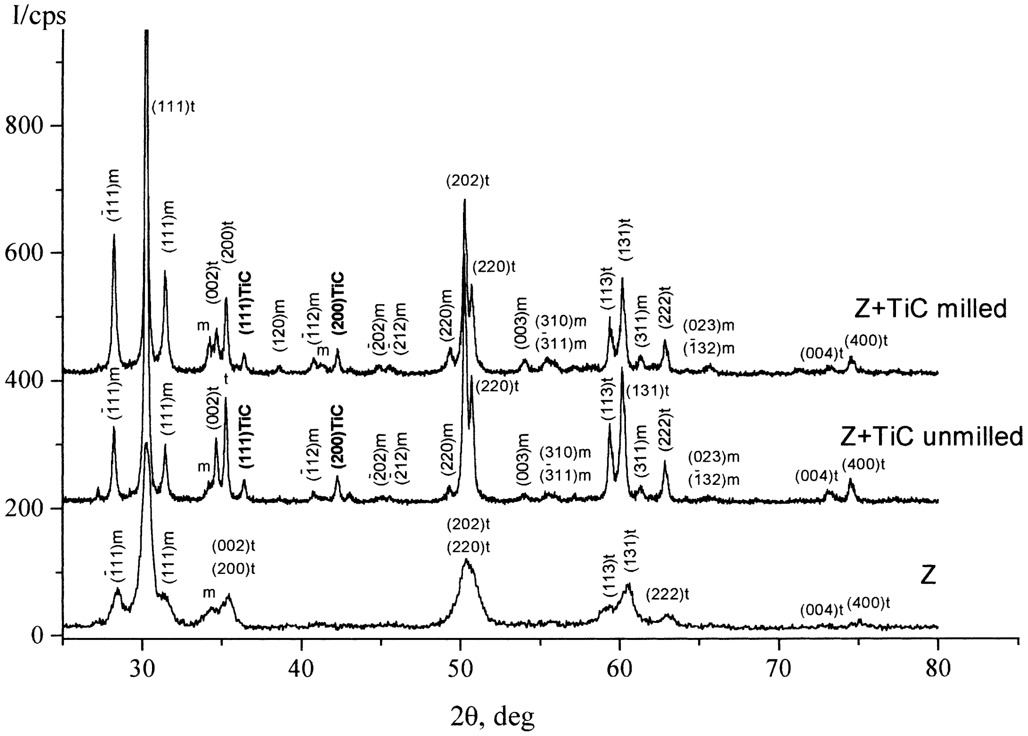

Fig. 3. X-ray diffraction patterns of the original Z powder and the Z + TiC composite powder before and after attrition milling for 2 h.

available in the system is reacted. The increased specific surface area of Z + TiC can be attributed to some amount of non-reacted amorphous carbon. This hypothesis was confirmed by DTA-TG measurements performed in air. The DTA curve of the Z + TiC powder (Fig. 4) shows two exothermic peaks: one at 511 °C and another one at 638 °C. A weight increase of the sample accompanies the first peak. This was due to the oxidation reaction of TiC. X-ray analysis of the sample heated to the peak temperature in air revealed the presence of TiO_2 (anatase).

A weight decrease accompanies the second peak observed in the DTA curve, shown in Fig. 4. This can be attributed to the oxidation reaction of non-reacted carbon. Overlapping of the two exothermic peaks, which occurred also if a heating rate of 2 °C/min has been used, made impossible to calculate with good precision both of the TiC content on the basis of the sample weight increase and non-reacted carbon content on the basis of the sample weight decrease. In the latter case, an estimation indicated the value larger than 6.3 wt.%.

The attrition milling of the Z + TiC composite powder brought about an increase in the content of the monoclinic phase (Table 1).

In order to create conditions for further reaction of the non-reacted carbon with titanium, one part of the Z + TiC powder has been diluted with three parts of the powder Z. The mixture was used to prepare sintered bodies as mentioned earlier.

3.2. Characteristics of the sintered bodies

The phase composition of the sintered bodies, obtained from the starting powder Z and the composite powder Z + TiC diluted with Z, is shown in Fig. 5. The zirconia solid solutions of tetragonal and monoclinic symmetry and additionally the TiC phase, in case of the 25% Z + TiC–75% Z material, were detected. The

Table 2
Phase composition of the sintered materials

Sample	V_m, vol.%	V_t, vol.%	V_t/V_m	V_{TiC}, vol.%	W_{TiC}, wt.%
Z, 1400 °C	51.7±0.5	48.3±0.5	0.93	0	0
Z, 1500 °C	56.8±0.4	43.2±0.4	0.76	0	0
25% Z + TiC–75% Z, 1400 °C	61.5±0.7	24.9±0.1	0.40	13.6±0.8	11.4±0.7
25% Z + TiC–75% Z, 1500 °C	40.3±0.3	47.0±0.2	1.17	12.7±0.9	10.7±0.7

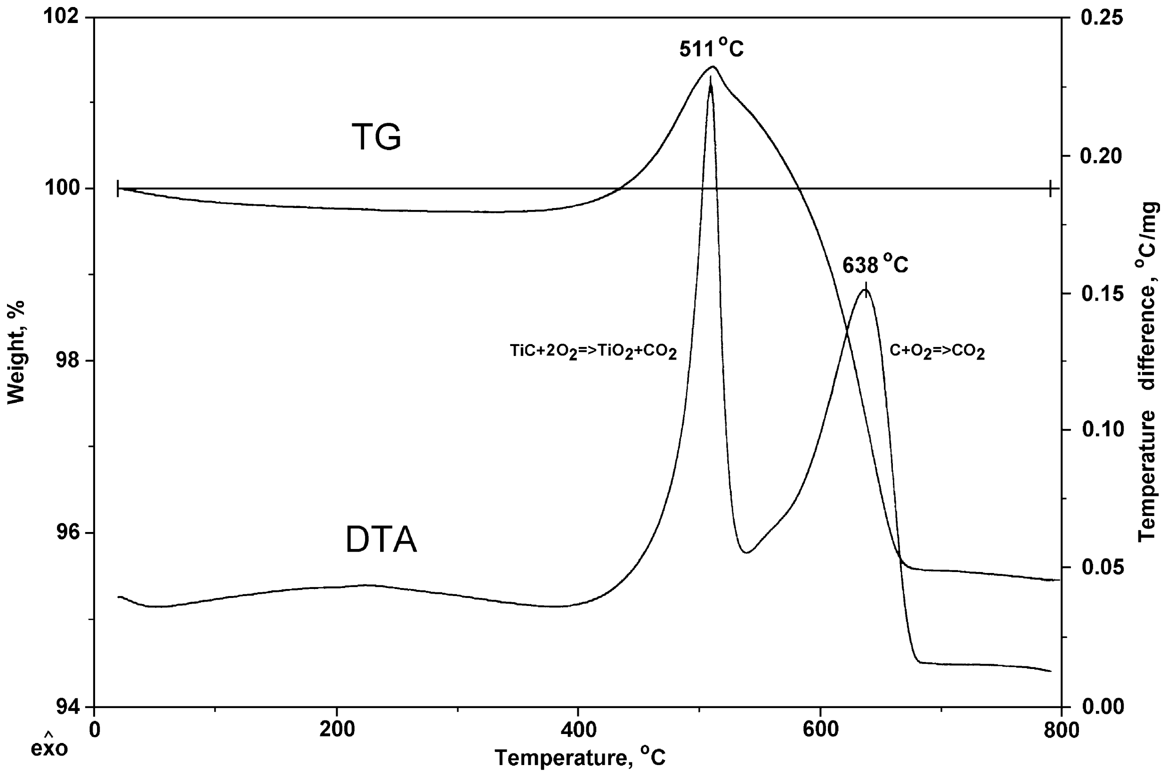

Fig. 4. DTA and TG curves of the Z + TiC powder (10 °C/min, air).

tetragonal phase content in the composites derived from the Z + TiC powder was closely connected to their density (compare Tables 2 and 3). The best densification (96% of theoretical density) has been found for the composite sintered at 1500 °C. It showed also the highest ratio of the tetragonal to monoclinic phases content (1.17). Within the limits of the measurement error, the TiC content remained unchanged with the sintering temperature and reached the value of ~11 wt.%. This value is significantly larger than that shown by the starting 25% Z + TiC–75% Z mixture (2.3 wt.%). This proves the continuous reaction of non-reacted carbon with titanium, derived from the matrix zirconia solid solution. The presence of the non-reacted carbon impeded densification of the mixture at 1400 °C, however improved its densification at 1500 °C when compared to the starting powder Z sintered at the same temperatures. This was most probably connected with an improvement in the pore size distribution due to both mixing the powders of different morphology (see Fig. 2) and the TiC formation reaction and a reduction in differential densification. Consequently, a larger fraction open porosity was maintained to higher sintered density, thereby reducing normal and abnormal grain growth rates, and pore breakaway. The reduction of grain growth has been observed indeed (see Fig. 6). The increased density with combination with the increased tetragonal phase content and the presence of TiC inclusions improved mechanical properties of the composite sintered at 1500 °C, especially with respect to its hardness (Table 3).

The value of the parameter x depicting the deviation from stoichiometry of TiC_{1-x} can be assessed using the measured cell parameter, a, of the phase and the dependence of lattice parameter on the carbon vacancy concentration presented e.g. by Fryt [18]. Table 4 contains the assessed a and x values for the TiC inclusions synthesized in situ and, for comparison, those for reference TiC used in X-ray phase analysis. The data

Table 3
Properties of the sintered materials

Sample	Sintering temperature (°C)	Apparent density (g/cm^3)	HV (GPa)[a]	K_{Ic} (MPam$^{0.5}$)[a]
Z	1400	5.39±0.02	8.0±0.3	3.4±0.1
Z	1500	5.42±0.04	Broken sample	Broken sample
25% Z + TiC–75% Z	1400	4.09±0.31	4.8±0.2	3.0±0.1
25% Z + TiC–75% Z	1500	5.64±0.05	11.2±0.6	4.6±0.1

[a] *HV* and K_{Ic} was measured under a load of 196 N and a loading time of 10 s.

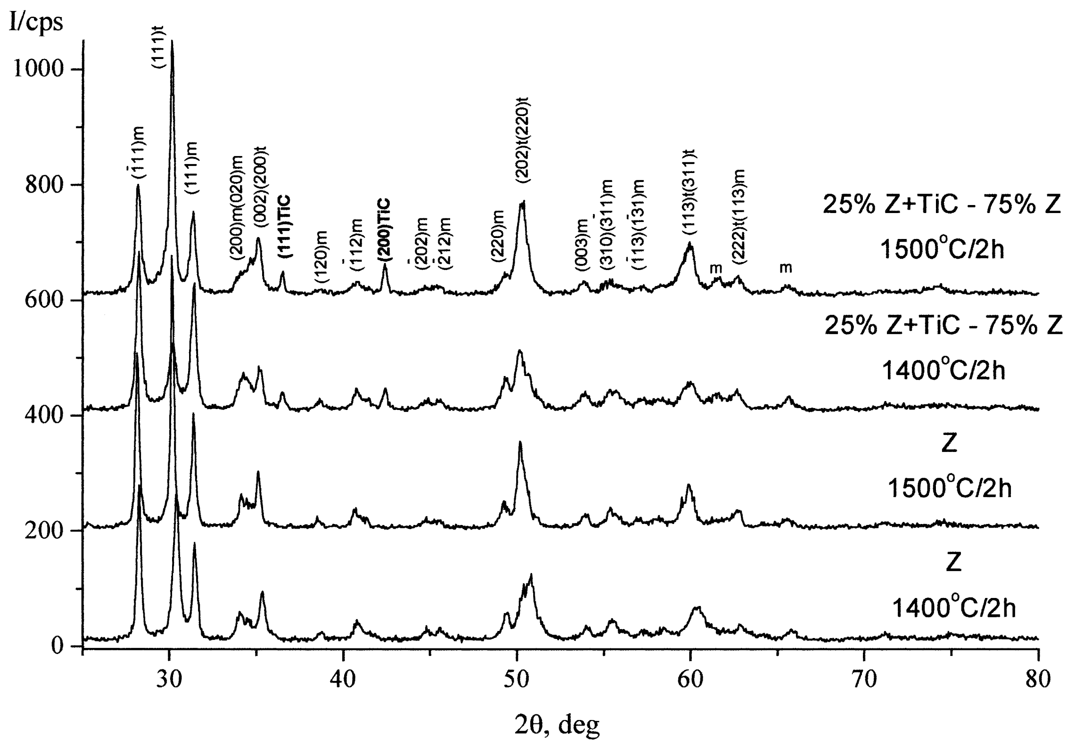

Fig. 5. X-ray diffraction patterns of the materials derived from the Z powder without and with addition of the Z + TiC composite powder after sintering in argon at indicated temperatures.

indicate very large deviation from stoichiometry of the titanium carbide phase obtained by means of the reaction of carbon and titanium extracted from the zirconia solid solution. Within the limits of the measurement error, the deviation is of the order of the highest possible one (0.535 [19]). The reference TiC showed smaller than TiC in situ but a large value of the deviation from stoichiometry.

The addition of Z + TiC to Z influenced the microstructure of the resultant composites. As shown in Fig. 6a and b, intensive grain growth, observed in case of the material derived from the Z powder, was limited and the microstructure of the composite was uniform, fine grained, and dense. Majority of the TiC particles had the form of intergranular oval inclusions of 100–400 nm in size as indicated by comparison of Fig. 6b and c. In some areas, colonies of nanocrystalline elongated TiC inclusions were observed (Fig. 6c). Morphologically similar inclusions have been found within the carburised surface layer of dense Ti,Y–TZP material [15]. This suggests that the colonies of the elongated TiC inclusions were formed during sintering in the reaction of titanium originated from zirconia solid solution and non-reacted carbon supplied by the powder Z. The dense aggregates of crystallites of Y_2O_3–TiO_2–ZrO_2 solid solution should take part in this process. On the contrary, the oval TiC inclusions originated from the titanium carbide introduced by the Z + TiC powder.

3.3. *The role of oxygen vacancies in the TiC formation*

The perfect densification and the lack of pores were the characteristic feature of areas, in which the colonies of the elongated TiC inclusions were observed. The surface layers containing TiC grown in situ during carburising the dense Ti,Y–TZP materials had similar features [15]. The above observations are rather difficult to interpret in terms of the TiC formation process accompanied by the CO evolution in the vicinity of the

Table 4
Average values of cell parameter, *a*, and deviation from stoichiometry, *x*, of TiC synthesized in situ and reference TiC used in X-ray phase analysis

	TiC_{1-x} in situ	TiC_{1-x} reference
a (nm)	0.4267±0.0027	0.4315±0.0002
x	0.69±0.17	0.39±0.01

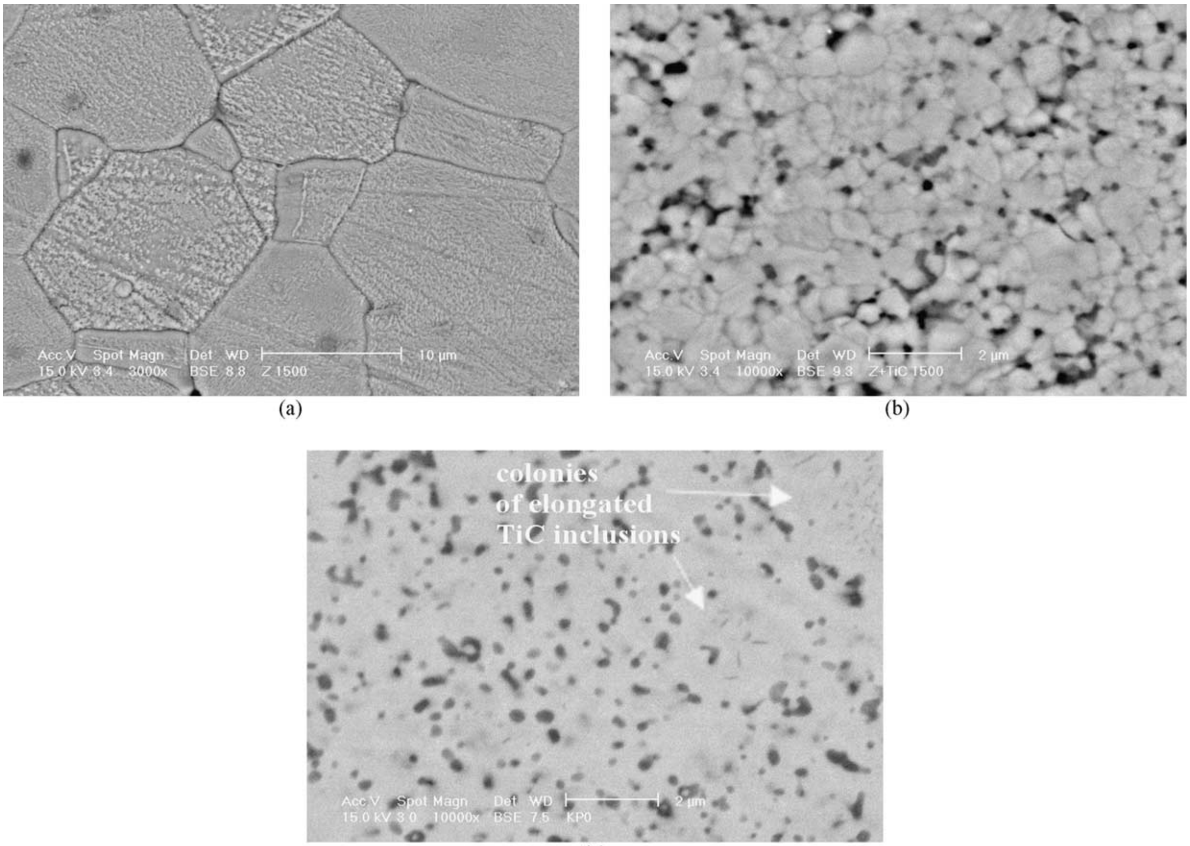

(a) (b)

(c)

Fig. 6. SEM microphotographs (a) Z derived material sintered for 2 h at 1500 °C, (b) 25% Z + TiC–75% Z composite sintered for 2 h at 1500 °C, (c) back scattered image of the sample shown in (b). TiC inclusions are represented by oval or elongated spots darker than the background in the back scattered images as indicated by EDS chemical analysis. The samples (a) and (b) were thermally etched for 2 h at 1300 °C in vacuum.

growing TiC phase which is the potential source of porosity. Therefore, another mechanism is proposed. Analysing the overall Eq. (1) one can state that it summarizes the effect of two processes described by the following tentative equations:

$$TiO_2(s) + C(s) \leftrightarrow TiC(s) + O_2(g)$$

$$O_2(g) + 2C(s) \leftrightarrow 2CO(g) \qquad (5)$$

The first process corresponds to the disappearance of the titanium and oxygen sites in the TiO_2 structure and with the formation of TiC and gaseous oxygen due to the reaction with carbon [Eq. (4)]. The second one is the reaction of the evolved oxygen with carbon to produce CO [Eq. (5)].

There are some differences between carbothermal reduction of bulk TiO_2 and the carbothermal reduction of titanium originated from zirconia solid solution. The former process concerns the case of two solid phases separated from the beginning of the process over an interface in which the reaction zones arise. The in situ formation of TiC in the Y_2O_3–TiO_2–ZrO_2 solid solution concerns a different situation because the titanium ions are dispersed at the atomic scale and the titanium phase is not marked off. Therefore, a limited amount of titanium is available for the reaction with the carbon particle contacted with the zirconia solid solution grain. It causes a limited probability of the TiC nucleus formation and, as a result, small number of the TiC nuclei can be formed. The resultant reaction front is discontinuous as opposed to the continuous front reaction in the case of the reaction of bulk TiO_2 with carbon. The only possibility of growth of the TiC nuclei is to grow into the zirconia solid solution in a form of separated and elongated particles. Most probably, in case of dense polycrystalline systems such as an aggregate of crystallites or carburised surface of a sintered body, mainly grain boundaries take part both in the nucleation and growth process. This suggestion is supported by the observation reported by Kowalski et al. [19] showing that the grain boundary diffusion is faster than the bulk diffusion by about 5 orders of magnitude in the case of the diffusion of titanium in the yttria fully stabilized zirconia.

As the carbon diffusion in TiC_{1-x} is about three orders of magnitude faster than the titanium diffusion [18], the growth process of the TiC inclusions should occur at the interface boundary between TiC and zirconia solid solution. The process utilises the flux of titanium ions originating from the surrounding zirconia solid solution and the one of carbon atoms diffusing through the TiC inclusion, as shown schematically in Fig. 7.

It is assumed that the structure of the dense yttria–titania–zirconia solid solution makes the formation of the CO particles in vicinity of the growing TiC nucleus difficult due to the stresses which arises in the process. So, the reaction expressed by the Eq. (5) is shifted to the free surface of the zirconia solid solution after a diffusion transport of oxygen through the zirconia lattice. The coupled diffusions of oxygen ions and oxygen vacancies take place in the process (Fig. 7).

In the case of the yttria–titania–zirconia solid solution at the applied sintering temperature, the concentration of the oxygen vacancies is very high which creates an easy way to "transport oxygen sites" from the reaction zone to the free surface. Three processes are responsible for the high concentration of the oxygen vacancies: (i) substitution of zirconium cations by trivalent cation of yttrium, (ii) reduction of Ti^{4+} to Ti^{3+} at low oxygen partial pressure, (iii) deoxidation of zirconia at low oxygen partial pressure. The appropriate defect reactions can be expressed by the following quasi-chemical equations:

$$Y_2O_3 \rightarrow 2Y'_{Zr} + V_O^{\bullet\bullet} + 3O_O^x \qquad (6)$$

$$2Ti_{Zr}^x + O_O^x \leftrightarrow 2Ti'_{Zr} + V_O^{\bullet\bullet} + \tfrac{1}{2}O_2(g) \qquad (7)$$

$$2Zr_{Zr}^x + O_O^x \leftrightarrow 2Zr'_{Zr} + V_O^{\bullet\bullet} + \tfrac{1}{2}O_2(g) \qquad (8)$$

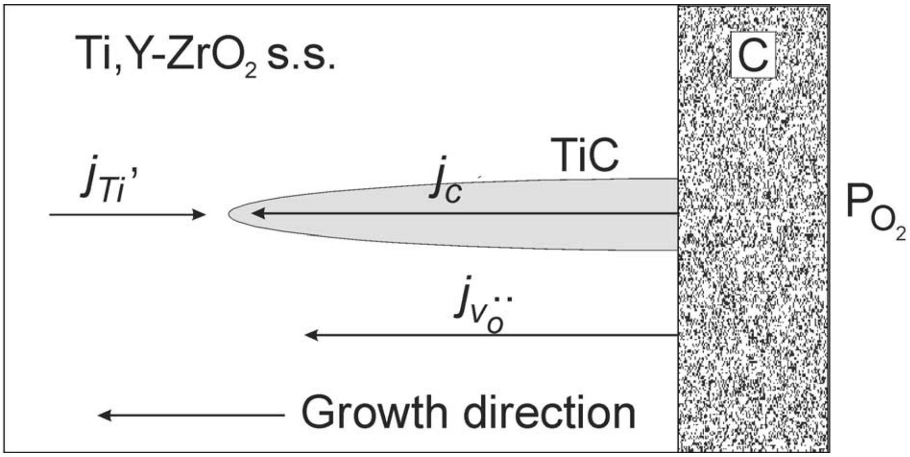

Fig. 7. Scheme of the TiC in situ formation process. (*j*—flux of appropriate component, P_{O_2}—oxygen partial pressure).

where: $V_O^{\bullet\bullet}$ indicates a doubly charged oxygen vacancy, $\mathrm{Y}'_{\mathrm{Zr}}$ indicates yttrium on the zirconium site with a formal charge of −1, $\mathrm{Ti}'_{\mathrm{Zr}}$ indicates Ti^{3+} on the zirconium site, $\mathrm{Zr}'_{\mathrm{Zr}}$ indicates the localized electron on a zirconium site, $\mathrm{O}_{\mathrm{O}}^{x}$ indicates normal oxygen on an oxygen site, $\mathrm{Zr}_{\mathrm{Zr}}^{x}$,$\mathrm{Ti}_{\mathrm{Zr}}^{x}$ indicates the zirconium (IV) and titanium (IV) ion on a zirconium site, respectively.

Using the above notation, the equations expressing the reaction of Ti^{3+} and Ti^{4+} ions with carbon atoms and a simultaneous process of vacancy annihilation, due to taking over oxygen ions from the oxygen sites which disappear, can be written as follows:

$$\mathrm{Ti}'_{\mathrm{Zr}} + 3\mathrm{Zr}'_{\mathrm{Zr}} + 2\mathrm{V}_{\mathrm{O}}^{\bullet\bullet} + 6\mathrm{O}_{\mathrm{O}}^{x} + \mathrm{C} = \mathrm{TiC} + 3\mathrm{Zr}_{\mathrm{Zr}}^{x} + 6\mathrm{O}_{\mathrm{O}}^{x} \tag{9}$$

$$\mathrm{Ti}_{\mathrm{Zr}} + 4\mathrm{Zr}'_{\mathrm{Zr}} + 2\mathrm{V}_{\mathrm{O}}^{\bullet\bullet} + 8\mathrm{O}_{\mathrm{O}}^{x} + \mathrm{C} = \mathrm{TiC} + 4\mathrm{Zr}_{\mathrm{Zr}}^{x} + 8\mathrm{O}_{\mathrm{O}}^{x} \tag{10}$$

A decreased vacancy concentration in the vicinity of TiC inclusion when compared to the balance value in other regions of the system is an obvious result of the TiC formation expressed by Eqs. (9) and (10). In this way a gradient of vacancy concentration arises and it is compensated easily by the oxygen vacancy diffusion from the free surface to the TiC inclusion. This is accompanied by the oxygen diffusion in the opposite direction. The oxygen transferred to the free surface of the zirconia solid solution grains reacts with carbon to form CO satisfying requirements of Eq. (1). It must be emphasized that the free surface is the constant source of the oxygen vacancies. On this surface a balance value of the oxygen vacancy concentration is established depending on the oxygen partial pressure in the surrounding atmosphere as it is described by Eqs. (7) and (8).

On the present state of the studies it is not possible to say whether the proposed mechanism takes part in the formation of the oval TiC inclusions in the zirconia matrix or not. The same concerns the TiC formation mechanism in the carburised ytrria–titania–zirconia powders. However, one should assume that the proposed mechanism generally operates during the TiC crystallisation within the carburised zirconia solid solutions doped with titania.

4. Conclusions

The presented work shows that dense zirconia nanocomposites with a fine grained microstructure can be pressurelessly sintered in argon using a powder which contains synthesized in situ TiC and carbon. The latter one gives the possibility to crystallize elongated TiC inclusions during sintering. The TiC inclusions introduced into the system with the starting powder displayed an oval shape after sintering. Both categories of TiC inclusions were nanometric in size and showed a large deviation from stoichiometry. The presence both of TiC crystallised in situ and carbon in the zirconia powder led to reduced grain growth and improvement of the mechanical characteristics of the zirconia materials. The proposed mechanism of the in situ formation of the elongated TiC inclusions which utilizes the current knowledge on the transport properties of oxygen vacancies in the oxygen sublattice of the zirconia solid solution explains satisfactorily the experimental observations.

Acknowledgements

The author thanks Dr. M. M. Bućko for many helpful discussions and Dr. M. Faryna for SEM back scattered images. The work was supported by the Polish Committee for Scientific Research under the grant no PBZ/KBN-013/T08/36.

References

[1] N. Claussen, K. Weiskopf, M. Rühle, Tetragonal zirconia polycrystals reinforced with SiC whiskers, J. Am. Ceram. Soc. 68 (1986) 288–292.

[2] M. Poorteman, P. Descamps, F. Cambier, J. Leriche, B. Thierry, Hot isostating pressing of SiC-platelets/Y-TZP, J. Eur. Ceram. Soc. 12 (1993) 103–109.

[3] G.Y. Lin, T.C. Lei, S.X. Wang, Y. Zhou, Microstructure and mechanical properties of SiC whisker reinforced $\mathrm{ZrO_2}$ (2 mol% $\mathrm{Y_2O_3}$) based composites, Ceram. Int. 22 (1996) 199–205.

[4] Zh. Ding, R. Oberacker, F. Thummler, Microstructure and mechanical properties of yttria stabilized tetragonal zirconia polycrystals (Y–TZP) containing dispersed silicon carbide particles, J. Eur. Ceram. Soc. 12 (1993) 377–383.

[5] K. Haberko, Z. Pędzich, G. Róg, M.M. Bućko, M. Faryna, The TZP matrix—WC particulate composites, Eur. J. Solid State Inorg. Chem. 32 (1995) 593–601.

[6] Z. Pędzich, K. Haberko, J. Piekarczyk, M. Faryna, L. Lityñska, Zirconia matrix–tungsten carbide particulate composites manufactured by hot-pressing technique, Mater. Lett. 36 (1998) 70–75.

[7] Z. Pędzich, K. Haberko, J. Babiarz, M. Faryna, The TZP-chromium oxide and chromium carbide composites, J. Eur. Ceram. Soc. 18 (1998) 1939–1944.

[8] M. Fukuhara, Properties of (Y)$\mathrm{ZrO_2}$–$\mathrm{Al_2O_3}$–(Ti or Si)C composites, J. Am. Ceram. Soc. 72 (2) (1989) 236–242.

[9] G.-D. Zhan, T.-R. Lai, J.-L. Shi, T.-S. Yen, Y. Zhou, Y.-Z. Zhang, Microstructure and mechanical properties of yttria stabilized tetragonal zirconia polycrystals containing dispersed TiC particles, J. Mater. Sci. 31 (1996) 2903–2907.

[10] J. Vleugels, O. Van Der Biest. $\mathrm{ZrO_2}$–TiX composites, in: Key Engineering Materials, Vols. 132–136, Part 3, Trans Tech Publications, Switzerland, 1997, pp. 2064–2067.

[11] W. Pyda, TiC inclusions synthesized in-situ in the zirconia matrix, in: S. Adali, E.V. Morozov, V.E. Verijenko (Eds.), Pro-

ceedings of the 2nd International Conference on Composite Science and Technology, Department of Mechanical Engineering, University of Natal, Durban, 1998, pp. 195–200.

[12] K. Haberko, W. Pyda, Z. Pędzich, M.M. Bućko, A TZP matrix composite with in situ grown TiC inclusions, J. Eur. Ceram. Soc. 20 (2000) 2649–2654.

[13] J. Liu, J. Li, H. Wang, Y. Huang, In situ synthesis of yttria-stabilized tetragonal zirconia polycrystalline powder containing dispersed titanium carbide by selective carbonisation, J. Am. Ceram. Soc. 82 (1999) 1611–1613.

[14] G. Róg, Thermodynamics of the reaction of the carbide and nitride formation in the ZrO_2–Y_2O_3–TiO_2 s.s. at different atmospheres, in particulate composites with ZrO_2 matrix, in: Report for the Polish Committee for Scientific Research, grant No. PB/964/7/91, Department of Materials Science and Engineering, University of Mining and Metallurgy, Cracow, 1994, chapter II.

[15] K. Haberko, A. Wajler, M.M. Bućko, Z. Pędzich, M. Faryna, W. Pyda, J. Piekarczyk, Effect of carbon treatment on surface hardening of TiY–TZP, Ceram. Int. 28 (2002) 553–556.

[16] D.L. Porter, A.H. Heuer, Microstructural development in MgO-partially stabilised zirconia (Mg—PSZ), J. Am. Ceram. Soc. 62 (5–6) (1979) 298–305.

[17] K.A. Niihara, A fracture mechanics analysis of indentation-induced Palmqvist crack in ceramics, J. Mater. Sci. Lett. 2 (1983) 221.

[18] E.M. Fryt, Defect mobility in TiC_{1-x} at high temperatures, Solid State Ionics 101–103 (1997) 437–443.

[19] K. Kowalski, A. Bernasik, A. Sadowski, Bulk and grain boundry diffusion of titanium in yttria-stabilized zirconia, J. Eur. Ceram. Soc. 20 (2000) 951–958.